Optimum Detection of an Optical Image O
a Photoelectric Surface

Carl W. Helstrom and Lily Wang*

Department of Applied Physics and Information Science
University of California, San Diego
La Jolla, California 92037

ABSTRACT

The detection of an optical image in the presence of uniform background light is based on a likelihood ratio formed of the numbers of photoelectrons emitted from small elements of a photoelectric surface onto which the image is focused. When diffraction is negligible and the surface has unit quantum efficiency, this detector is equipollent with the optimum detector of the image-forming light. Its performance is compared with that of the threshold detector and that of a detector basing its decisions on the total number of photoelectrons from a finite area of the image. The illuminance of the image is postulated to have a Gaussian spatial distribution. All three detectors exhibit nearly the same reliability.

*This research has been carried out under Grant NGL 05-009-079 from the National Aeronautics and Space Administration.

32 p.

1. The Ideal Photoelectric Detector

An optical detector is to decide whether a certain luminous object is present or not in an object plane at a distance R from its aperture. The aperture contains a lens focusing the object plane onto an image plane I at distance R_1 behind it. The image plane consists of a photoelectrically emissive surface divided like a mosaic into a large number of small areas δA_I, and the numbers n_i of photoelectrons emitted from these during an observation interval of duration T constitute the primary data on which is based the decision about the presence or absence of the object sought. In general, background light also enters the aperture, and an observer is to choose between two hypotheses: (H_0) only background light is present, and (H_1) besides the background light, light from the object is also incident on the aperture.

Let the illuminance at point $\underset{\sim}{x}$ of the image plane caused by background light in the frequency interval ν to $\nu + d\nu$ be $J_0(\underset{\sim}{x},\nu)d\nu$, and let the illuminance under hypothesis H_1 be

$$J_1(\underset{\sim}{x},\nu)d\nu = J_s(\underset{\sim}{x},\nu)d\nu + J_0(\underset{\sim}{x},\nu)d\nu, \qquad (1)$$

where $J_s(\underset{\sim}{x},\nu)d\nu$ is the illuminance produced by the light from the object sought (the 'signal'). Let $\eta(\nu)$ be the quantum efficiency of the photoelectric surface at frequency ν. We assume that the duration T of the observation interval is so much greater than the reciprocal bandwidth W^{-1} of the object light that the numbers n_i of photoelectrons from the various elements of the image plane are statistically independent Poisson-distributed

random variables with mean values

$$n_{ik} = \underset{\sim}{E}(n_i|H_k) = T \int_{A_i} \int_0^\infty \eta(\nu)\ J_k(\underset{\sim}{x},\nu) d^2\underset{\sim}{x}\ d\nu/h\nu$$

$$\doteq M_k(\underset{\sim}{x}_i)\ \delta A_I, \quad k = 0,\ 1, \tag{2}$$

where A_i, centered at $\underset{\sim}{x}_i$, is the i-th element of the image plane I, on which $d^2\underset{\sim}{x}$ is an element of integration, h is Planck's constant, and

$$M_k(\underset{\sim}{x}) = T \int_0^\infty \eta(\nu)\ J_k(\underset{\sim}{x},\nu) d\nu/h\nu. \tag{3}$$

Ordinarily $M_0(\underset{\sim}{x})$ is constant over the part of the surface I where the object is imaged. When the image sought is quasimonochromatic, the incident light will have been filtered to remove as much as possible of the background outside the frequency band of the image.

The optimum strategy for deciding between the two hypotheses compares the statistic[1]

$$g = \sum_i n_i\ \ell n(n_{i1}/n_{i0}) = \sum_i n_i\ \ell n \left[\frac{M_1(\underset{\sim}{x}_i)}{M_0(\underset{\sim}{x}_i)}\right] \tag{4}$$

with a decision level g_0; the system will choose H_1 if $g > g_0$ and H_0 if $g \leq g_0$. This statistic differs from the logarithm of the likelihood ratio by a constant,

$$\ell n\ \Lambda(\{n_i\}) = g - \sum_i (n_{i1} - n_{i0}) = g - N_s, \tag{5}$$

where

$$N_s = \int_I M_s(\underset{\sim}{x}) d^2\underset{\sim}{x}, \quad M_s(\underset{\sim}{x}) = M_1(\underset{\sim}{x}) - M_0(\underset{\sim}{x}), \tag{6}$$

is the total average number of photoelectrons ejected by the light from the object.

The performance of the detector can be characterized by the false-alarm probability

$$Q_0 = \Pr\{g > g_0 | H_0\} = 1 - P_0(g_0) \tag{7}$$

and the detection probability

$$Q_d = \Pr\{g > g_0 | H_1\} = 1 - P_1(g_0). \tag{8}$$

Here $P_0(g)$ and $P_1(g)$ are the cumulative distributions of the statistic g under the two hypotheses. When hypothesis H_0 has prior probability ζ and H_1 prior probability $1 - \zeta$, the average probability of error is

$$P_e = \zeta Q_0 + (1-\zeta)(1 - Q_d), \tag{9}$$

and it is minimum when the decision level g_0 is[2]

$$g_0 = N_s + \ell n[\zeta/(1 - \zeta)]. \tag{10}$$

Under the Neyman-Pearson criterion g_0 is set to yield a pre-assigned

false-alarm probability Q_0.

The distribution functions $P_0(g)$ and $P_1(g)$ can be derived from the moment-generating functions (m.g.f.'s) $h_0(s)$ and $h_1(s)$, which are the Laplace transforms of the probability density functions (p.d.f.'s) of g and are given in the limit $\delta A_I \to 0$ by[1]

$$h_k(s) = \int_{0-}^{\infty} e^{-sg}\, dP_k(g)$$
$$= \exp\left\{ -\int_I M_k(\underset{\sim}{x}) \left\{ 1 - \left[\frac{M_1(\underset{\sim}{x})}{M_0(\underset{\sim}{x})} \right]^{-s} \right\} d^2\underset{\sim}{x} \right\}, \quad k = 0, 1, \tag{11}$$

the integral being taken over the entire image plane I. Because of (5), or as can be shown directly,

$$h_1(s) = \exp(-N_s)\, h_0(s - 1). \tag{12}$$

If $M_s(\underset{\sim}{x}) \equiv 0$ outside a finite area I' of the image plane, the optimum detection statistic involves only emissions within that area, and there is a finite probability

$$\Pr\left\{ g = 0 \middle| H_k \right\} = \exp\left\{ -\int_{I'} M_k(\underset{\sim}{x}) d^2\underset{\sim}{x} \right\}, \quad k = 0, 1, \tag{13}$$

that no photoelectrons will be emitted there at all. The p.d.f.'s of g then have a delta-function at g = 0.

If both $M_0(\underset{\sim}{x})$ and $M_s(\underset{\sim}{x})$ are constant over I', the statistic $g[\ell n(M_1/M_0)]^{-1}$ has only integral values with a Poisson distribution under both hypotheses. When the Neyman-Pearson criterion is being used, a

desired false-alarm probability is set, and randomization may be necessary. The detection probability versus the mean total number N_s of photoelectrons ejected by the object light has been calculated and graphed elsewhere.[3]

In this paper we shall study the evaluation of the error probabilities and compare the performance of the optimum detector with two other, simpler detectors. One is the threshold detector, which utilizes a normalized form of the statistic

$$g' = \sum_i n_i M_s(\underset{\sim}{x}_i)/M_0(\underset{\sim}{x}_i).$$

The other detector simply counts all the electrons emitted from a finite area of the image plane.

2. Relation to the Optimum Receiver

The photoelectric detector just described represents a particular way of processing the light field at the aperture A of the optical system in order to choose between the two hypotheses. It should be compared with the optimum means of processing that field. We suppose that the object plane radiates incoherent, quasimonochromatic light uniformly distributed in a frequency band of width W about the central frequency $\bar{\nu}$, $W << \bar{\nu}$. The total radiance at point $\underset{\sim}{u}$ of the object plane under hypothesis H_1 is $B(\underset{\sim}{u})$; under H_0 it is zero. Under both hypotheses thermal background light of effective absolute temperature $\mathscr{T}$ is also incident on the aperture. It is broadly distributed in direction and possesses a Planck distribution in frequency.

The field at the aperture is considered classically as a scalar spatio-temporal complex Gaussian random process. In order to formulate the optimum decision strategy this field is broken up into spatial modes much as a purely temporal signal is treated by the Karhunen-Loève expansion.[4,5] The fraction $h_{\underset{\sim}{p}}$ of the object light in the $\underset{\sim}{p}$-th spatial mode is the $\underset{\sim}{p}$-th eigenvalue of the integral equation

$$h_{\underset{\sim}{p}}\, \eta_{\underset{\sim}{p}}(\underset{\sim}{r}_2) = (AB_T)^{-1} \int_A \beta(\underset{\sim}{r}_2 - \underset{\sim}{r}_1)\eta_{\underset{\sim}{p}}(\underset{\sim}{r}_1)d^2\underset{\sim}{r}_1, \tag{14}$$

where A is the area of the aperture A and the kernel $\beta(\underset{\sim}{r})$ is the spatial coherence function of the object light at the aperture. It is the spatial Fourier transform of the radiance distribution $B(\underset{\sim}{u})$ of the object,

$$\beta(\underset{\sim}{r}) = \int_0 B(\underset{\sim}{u})\exp(ik\underset{\sim}{u} \cdot \underset{\sim}{r}/R)d^2\underset{\sim}{u}; \tag{15}$$

where $k = 2\pi/\lambda = 2\pi c/\bar{\nu}$ is the propagation constant, c = velocity of light, λ = wavelength. In (14)

$$B_T = \beta(\underset{\sim}{0}) = \int_0 B(\underset{\sim}{u})d^2\underset{\sim}{u} \tag{16}$$

is the total radiant power of the object.

The coefficient of the mode function $\eta_{\underset{\sim}{p}}(\underset{\sim}{r})$ in this expansion is a random function of time that is in turn expanded in temporal modes that are eigenfunctions of the temporal coherence function of the object light. The combination of a spatial and a temporal mode is called a spatio-temporal mode. When, as assumed here, the object light has a rectangular spectral

density of width W, and the product WT of that bandwidth and the observation time T is large, WT >> 1, there are approximately WT temporal modes each containing a fraction $(WT)^{-1}$ of the object light; the rest are negligible.[4]

Under the assumption that WT >> 1, quantum detection theory shows that the optimum strategy forms the statistic[6]

$$U = \sum_{\underset{\sim}{p}} [n_{\underset{\sim}{p}} \ln(1 + h_{\underset{\sim}{p}} \mathcal{N}_s/\mathcal{N}WT)] - \mathcal{N}_s , \tag{17}$$

where $n_{\underset{\sim}{p}}$ is the total number of photons in the WT significant temporal components of the spatial mode $\underset{\sim}{p}$, $\mathcal{N}_s$ is the mean total number of photons received at A from the object, and

$$\mathcal{N} = [\exp(h\bar{\nu}/K\mathcal{T}) - 1]^{-1} \tag{18}$$

is the mean number of thermal photons per spatio-temporal mode of the aperture field, as given by the Planck law; K is Boltzmann's constant. The number $n_{\underset{\sim}{p}}$ has a Poisson distribution with mean values

$$\begin{aligned} \underset{\sim}{E}(n_{\underset{\sim}{p}}|H_0) &= \mathcal{N}WT, \\ \underset{\sim}{E}(n_{\underset{\sim}{p}}|H_1) &= h_{\underset{\sim}{p}} \mathcal{N}_s + \mathcal{N}WT, \\ \sum_{\underset{\sim}{p}} h_{\underset{\sim}{p}} &= 1, \end{aligned} \tag{19}$$

under the two hypotheses. Hypothesis H_1 is chosen if the statistic U exceeds a decision level U_0.

When the aperture A is rectangular, $a_x \times a_y$, with a_x and a_y much greater than the width of the kernel $\beta(\underset{\sim}{r})$ of (14), the eigenvalues $h_{\underset{\sim}{p}}$ are approximately

$$h_{\underset{\sim}{p}} \doteq \delta_x \delta_y B(p_x \delta_x, p_y \delta_y)/B_T, \quad \underset{\sim}{p} = (p_x, p_y),$$

$$\delta_x = \lambda R/a_x, \quad \delta_y = \lambda R/a_y. \tag{20}$$

The resolution lengths δ_x and δ_y in the object plane are much smaller than distances over which the radiance $B(\underset{\sim}{u})$ changes significantly. If the object is focused on the image plane, as in the detector of §1, the image is not visibly distorted by diffraction at the aperture, and if the imaging is otherwise perfect, the total illuminance it produces at point $\underset{\sim}{x}$ of the image plane I is

$$J_s(\underset{\sim}{x}) = CB(-R\underset{\sim}{x}/R_1) \tag{21}$$

for some constant C.

We can then write the statistic U as

$$U = \sum_{\underset{\sim}{p}} n_{\underset{\sim}{p}} \ell n \left[1 + \frac{M_s'(\underset{\sim}{x}_{\underset{\sim}{p}})}{M_0'}\right] - \mathcal{N}_s \tag{22}$$

if we put

$$M_0' = \mathcal{N}WT/\delta_x' \delta_y' = \mathcal{N}WTA/\lambda^2 R_1^2 , \tag{23}$$

$$M_s'(\underset{\sim}{x}) = \mathcal{N}_s J_s(\underset{\sim}{x}) \left[\int_I J_s(\underset{\sim}{x}) d^2\underset{\sim}{x}\right]^{-1} , \tag{24}$$

where

$$\delta_x' = \lambda R_1/a_x, \quad \delta_y' = \lambda R_1/a_y \tag{25}$$

are the resolution lengths in the image plane.

Comparing (22) with (4) we see that the optimum detection strategy handles the numbers $n_{\underset{\sim}{p}}$ of photons in the spatial modes in much the same way as the photoelectric detector handles the numbers of electrons ejected from the image plane. If we divided the image plane into insulated areas $\delta_x' \times \delta_y'$, and if the surface had unit quantum efficiency, the two detectors would be nearly the same.

The moment-generating functions of the statistic U are, under the two hypotheses,

$$h_0'(s) = \underset{\sim}{E}\left(e^{-sU}\middle|H_0\right)$$

$$= \exp\left\{s\mathcal{N}_s - \mathcal{N}WT \sum_{\underset{\sim}{p}} [1 - (1 + h_{\underset{\sim}{p}} \mathcal{N}_s/\mathcal{N}WT)^{-s}]\right\}, \tag{26}$$

$$h_1'(s) = \underset{\sim}{E}\left(e^{-sU}\middle|H_1\right) = h_0'(s - 1). \tag{27}$$

The number of degrees of freedom in the object is conveniently defined by[5]

$$M = \left(\sum_{\underset{\sim}{p}} h_{\underset{\sim}{p}}^2\right)^{-1} = AA_o/(\lambda R)^2 = A_o/\delta_x \delta_y , \tag{28}$$

where A_o is the effective area of the object, given by

$$A_o = B_T^2 \left[\int_0 [B(\underset{\sim}{u})]^2 d^2\underset{\sim}{u} \right]^{-1} . \tag{29}$$

When $M >> 1$, the m.g.f. in (26) is approximately

$$h_0'(s) = \exp\left\{ s\mathcal{N}_s - \mathcal{N}_{MWT} \int_0 \left\{ 1 - \left[1 + \frac{\mathcal{N}_s}{\mathcal{N}_{MWT}} \frac{B(\underset{\sim}{u})}{\overline{B}} \right]^{-s} \right\} d^2\underset{\sim}{u}/A_o \right\},$$

$$\overline{B} = B_T/A_o. \tag{30}$$

This result does not require the aperture to be rectangular, but follows from the two-dimensional counterpart of Theorem 1 of Chapter 5 of Grenander and Szegö;[7] for any function $f(x)$ analytic at $x = 0$,

$$\sum_{\underset{\sim}{p}} f(h_{\underset{\sim}{p}}) \doteq M \int_0 f(B(\underset{\sim}{u})/M\overline{B}) d^2\underset{\sim}{u}/A_o, \quad M >> 1, \tag{31}$$

as can be shown by expanding $f(h_{\underset{\sim}{p}})$ in powers of $h_{\underset{\sim}{p}}$ and using

$$\sum_{\underset{\sim}{p}} h_{\underset{\sim}{p}}^m = (AB_T)^{-m} \int_A \beta^{(m)}(\underset{\sim}{r}, \underset{\sim}{r}) d^2\underset{\sim}{r} , \tag{32}$$

where $\beta^{(m)}(\underset{\sim}{r}_1, \underset{\sim}{r}_2)$ is the m-th iterated kernel of (14) and is proportional to the Fourier transform of $[B(\underset{\sim}{u})]^m$ when $M >> 1$. The condition $M = A_o/\delta_x \delta_y >> 1$ means that the image is little distorted by diffraction, and if we assume perfect imaging we can use (21), (23), and (24) to write the m.g.f.'s as

$$h_k'(s) = \exp\left\{ s\mathcal{N}_s - \int_0 M_k'(\underset{\sim}{x}) \left\{ 1 - \left[1 + \frac{M_s'(\underset{\sim}{x})}{M_0'} \right]^{-s} \right\} d^2\underset{\sim}{x} \right\},$$

$$M_1'(\underset{\sim}{x}) = M_0' + M_s'(\underset{\sim}{x}), \quad k = 0, 1. \tag{33}$$

Comparing (33) and (11) we see that the optimum detection strategy yields the same performance as the optimum photoelectric detector when the quantum efficiency of the surface is $\eta = 1$ over the spectral band of the object light and diffraction by the aperture is negligible.

3. Performance of the Ideal Photoelectric Detector

a) Background Light Absent

When there is no background light, $M_0 \equiv 0$, no photoelectrons will be emitted under hypothesis H_0. Then under the Neyman-Pearson criterion a randomized strategy is required, with hypothesis H_1 chosen whenever any photoelectrons at all are observed; when none is emitted, H_1 is chosen with probability Q_0 and H_0 with probability $1 - Q_0$, where Q_0 is the pre-assigned false-alarm probability. The probability of detection is then

$$Q_d = 1 - (1 - Q_0)\exp(-N_s), \tag{34}$$

where as in (6) N_s is the mean number of photoelectrons ejected by light from the object.

When as in a binary communication system the Bayes criterion is adopted, with equal error costs and with prior probabilities ζ and $(1 - \zeta)$ for hypotheses H_0 and H_1, respectively, hypothesis H_1 is chosen whenever any photoelectrons at all are observed. When none is emitted, H_1 is chosen provided the likelihood ratio $\exp(-N_s)$ exceeds the ratio $A_0 = \zeta/(1 - \zeta)$; otherwise H_0 is chosen. The average probability of error is then

$$P_e = \min[\zeta, (1 - \zeta) \exp(-N_s)]. \tag{35}$$

When in particular the two hypotheses are equally likely,

$$P_e = \frac{1}{2} \exp(-N_s), \quad \zeta = \frac{1}{2}. \tag{36}$$

These error probabilities are independent of the distribution of image illuminance.

b) Background Light Present

The performance of the three detectors we are concerned with, the ideal photoelectric detector, the threshold detector, and the simple counter, will be assessed under the postulate that the object creates an image having the Gaussian form

$$M_s(\underset{\sim}{x}) = M_s(\underset{\sim}{0}) \exp(-\underset{\sim}{x}^2/2\Sigma^2) \tag{37}$$

with width Σ. This might be the image of a circular nebula or, more important, of a point source whose light has passed through a turbulent medium. When the turbulence can be pictured as occurring at one or a number of planes or 'phase screens', each introducing into the light a random phase shift represented by a two-dimensional Gaussian random process, the spatial coherence function $\beta(\underset{\sim}{r})$ at the aperture is simply multiplied by a factor $p(\underset{\sim}{r})$ that depends on the structure functions of the random phase shifts.[8] When these are quadratic functions of distance, or when there are many screens, the factor $p(\underset{\sim}{r})$ has approximately

a Gaussian form,

$$p(\underset{\sim}{r}) = \exp(-\underset{\sim}{r}^2/4L^2),$$

where L is a mean turbulence length that is the smaller, the more severe the turbulence. The image is the scaled Fourier transform of $p(\underset{\sim}{r})\ \beta(\underset{\sim}{r})$, and for a point source has the form given by (37) with the squared effective width

$$\Sigma^2 = \lambda^2 R_1^2/8\pi^2 L^2.$$

If the observation time T is much longer than the characteristic fluctuation time of the random phase shifts, the distributions of the numbers of emitted photoelectrons will still be of the Poisson variety. We can therefore use the m.g.f.'s given by (11), introducing the signal-to-noise ratio D^2 and the total effective number of background photoelectrons N_0 through

$$D^2 = N_s/N_0,$$

$$N_0 = 2\pi\ \Sigma^2\ M_0 = \eta \mathcal{N} WTA/4\pi L^2 \qquad (38)$$

where η is the average quantum efficiency over the spectral band of width W, T is the observation time, N_s is the mean total number of photoelectrons ejected by the image, and $\mathcal{N}$ is the mean number of background photons per mode, given by (18). We obtain from (11) the m.g.f.'s

$$h_k(s) = \exp\left\{ -N_0 \iint_I [1 + D^2 \exp(-\underset{\sim}{x}^2/2\Sigma^2)]^k \times \left\{ 1 - [1 + D^2 \exp(-\underset{\sim}{x}^2/2\Sigma^2)]^{-s} \right\} d^2\underset{\sim}{x}/2\pi\Sigma^2 \right\} =$$

$$= \exp\left\{ -N_0 \int_0^1 (1 + D^2 y)^k [1 - (1 + D^2 y)^{-s}] y^{-1} dy \right\}, \quad k = 0, 1, \tag{39}$$

after a change of integration variables and use of the circular symmetry of the integrand. The mean value and variance of the statistic g under each hypothesis can then be obtained by expanding the m.g.f.'s about s = 0,

$$\underset{\sim}{E}[g|H_k] = N_0 \int_0^1 (1 + k\, D^2 y) \ell n(1 + D^2 y) y^{-1}\, dy,$$

$$\mathrm{Var}[g|H_k] = N_0 \int_0^1 (1 + k\, D^2 y) \ell n^2(1 + D^2 y) y^{-1}\, dy, \quad k = 0, 1. \tag{40}$$

It is not generally possible to calculate the p.d.f.'s of the detection statistic g in closed form from m.g.f.'s such as those in (11) and (39). The logarithmic likelihood ratio g has what is known as an infinitely divisible distribution, but although there is a vast mathematical literature about such distributions, mostly concerned with limit theorems,[9,10] we have been unable to find there any specific advice about calculating the probability density functions. In a previous paper[1] a Gaussian approximation was used; it is valid only when $N_0 \gg 1$ and $D^2 \ll 1$. Farrell[11] recommended approximating the probability density function (p.d.f.) of the statistic g by a gamma distribution whose mean and variance match those of the true distribution as given by

(40).

As the m.g.f. is the Laplace transform of the p.d.f., it is natural to try evaluating the inverse Laplace transforms of $h_0(s)$ and $h_1(s)$ by the saddlepoint method. Daniels applied this method to finding the p.d.f. of the sample-mean statistic.[12] We have used it to obtain the cumulative distributions directly by evaluating the contour integral

$$1 - P_k(g) = \int_{\sigma - i\infty}^{\sigma + i\infty} [1 - h_k(s)]e^{gs}\, ds/2\pi is,$$

$$\sigma > 0, \quad k = 0, 1, \tag{41}$$

which can also be written

$$1 - P_k(g) = -\int_{\sigma - i\infty}^{\sigma + i\infty} h_k(s)e^{gs}\, ds/2\pi is,$$

$$\sigma < 0, \quad k = 0, 1, \tag{42}$$

by displacing the contour to the left of the origin. By an elaboration of the saddlepoint method, Rice produced an asymptotic expansion that is most suitable for numerical evaluation.[13,14]

The saddlepoint occurs at the values of s at which the phase

$$\phi_k(s) = \ell n\, h_k(s) + gs \tag{43}$$

of the integrand of (42) is stationary; it is the solution of the equation

$$\phi_k'(s) = h_k'(s)/h_k(s) + g = 0, \tag{44}$$

which from (39) yields

$$g = N_0 \int_0^1 (1 + D^2 y)^{k-s} \ln (1 + D^2 y) dy/y,$$

$$s = s_k, \quad k = 0, 1, \tag{45}$$

where the primes denote differention with respect to s. For the ideal photoelectric detector, by virtue of (12),

$$s_1 = s_0 + 1. \tag{46}$$

When $g > \underset{\sim}{E}(g|H_k)$, $s_k < 0$ and (42) is used; when $g < \underset{\sim}{E}(g|H_k)$, $s_k > 0$ and (41) is used. Rice's asymptotic expansion requires the values of the derivatives of the phase at the saddlepoint,

$$d^m\phi/ds^m = N_0 \int_0^1 (1 + D^2 y)^{k-s} \ln^m (1 + D^2 y) dy/y,$$

$$s = s_k, \quad m \geq 2, \quad k = 0, 1; \tag{47}$$

these were evaluated by numerical integration.

In Fig. 1 we have plotted the cumulative distributions of the statistic g under hypotheses H_0 and H_1 for a typical set of values of N_s and N_0, as calculated by the saddlepoint method and from the Gaussian and gamma-function approximations. The latter two approximations are least accurate in the tails of the distributions, and for small false-alarm probability Q_0 there may be a serious error in the decision level g_0 if

either is used.

Under the Neyman-Pearson criterion the false-alarm probability Q_0 is pre-assigned, and it is necessary to determine the decision level g_0 and the associated saddlepoint s_0. An iterative search method was used that took advantage of the fact that as s_0 becomes more negative, g_0 increases and Q_0 decreases. The behavior of the saddlepoint s_0 as a function of the signal-to-noise ratio D^2 is depicted in Fig. 2 for a typical case. The probability of detection Q_d is plotted as the solid curves in Figs. 3 and 4 as a function of the mean number N_s of received photons for various values of the mean number N_0 of background photons in an area $2\pi\,\Sigma^2$ concentric with the Gaussian image. In Fig. 5 is plotted the average probability P_e of error as calculated from (9) for the ideal detector when used in a binary communication system; $\zeta = \frac{1}{2}$ and $g_0 = N_s$.

4. The Threshold Detector

The structure of the optimum detector depends on the signal-to-noise ratio D^2, and if D^2 is unknown, the detector must be designed for some reasonable standard value. When D^2 is very small, the optimum detector is nearly equipollent to the threshold detector,[15] which is based on the term of lowest order in an expansion of the logarithm of the likelihood ratio in powers of D^2. For detecting an image on a photoelectric surface, the equivalent threshold statistic is[1]

$$g_\theta = \sum_i n_i\, m(\underset{\sim}{x}_i), \qquad m(\underset{\sim}{x}) = M_s(\underset{\sim}{x})/D^2 M_0(\underset{\sim}{x}), \tag{48}$$

which is compared with a decision level $g_{\theta 0}$, hypothesis H_1 being chosen when $g_\theta > g_{\theta 0}$. Its probability distributions under the two hypotheses can be determined from the m.g.f.'s

$$h_k^{(\theta)}(s) = \underset{\sim}{E}[\exp(-g_\theta s)\,|\,H_k]$$

$$= \exp\left\{-\int_I M_0(\underset{\sim}{x})[1 + D^2 m(\underset{\sim}{x})]^k \left\{1 - \exp[-sm(\underset{\sim}{x})]\right\} d^2\underset{\sim}{x}\right\},$$

$$k = 0, 1, \tag{49}$$

which for our Gaussian image in (37) becomes

$$h_k^{(\theta)}(s) = \exp\left\{-N_0 \int_0^1 (1 + D^2 y)^k (1 - e^{-sy}) y^{-1} dy\right\}$$

$$= \exp\left\{-N_0[C + \ell n\, s - Ei(-s) + kD^2(s - 1 + e^{-s})s^{-1}]\right\},$$

$$k = 0, 1, \tag{50}$$

where Ei(x) is the exponential integral and C = 0.577215... is Euler's constant. The derivatives needed for the asymptotic expansion resulting from the saddlepoint method can be written down in closed form,

$$d^m[\ell n\, h_k^{(\theta)}(s)]/ds^m = (-1)^m N_0 \int_0^1 y^{m-1} e^{-sy}(1 + D^2 y)^k\, dy$$

$$= (-1)^m N_0 \left\{s^{-m}[(m-1)! - \Gamma(m,s)] + kD^2 s^{-(m+1)}[m! - \Gamma(m+1,s)]\right\} \tag{51}$$

in terms of the incomplete gamma-function

$$\Gamma(m,x) = \int_x^\infty t^{m-1}\, e^{-t}\, dt = (m-1)!\, e^{-x} \sum_{r=0}^{m-1} x^r/r!. \quad (52)$$

The decision level $g_{\theta 0}$, which is independent of the signal-to-noise ratio, can be determined as described in Section 3, after which the detection probabilities are calculated by the asymptotic series derived from (41) and (42), into which $h_1^{(\theta)}(s)$ from (50) is substituted. The results are plotted as dashed curves on Figs. 3 and 4 for $N_0 = 0.5$ and $N_0 = 5$. They approach the detection-probability curves for the ideal photoelectric detector in an osculatory manner.

If the image detector is to be used in a binary communication system, the decision level minimizing the average probability of error P_e must be found from the likelihood ratio

$$dP_1(g_\theta)/dP_0(g_\theta) = \zeta/(1-\zeta), \quad g_\theta = g_{\theta 0},$$

and this requires finding the p.d.f.'s of g_θ by inverse Laplace transformation of (50), after which the minimum value of P_e is determined from (9). We have not carried through this calculation.

5. The Simple Counter

The simplest way to detect the image is to count all the photoelectrons emitted from a finite region of the image plane that is concentric with the expected image illuminance $J_s(\underset{\sim}{x})$. The total number n of

photoelectrons is then the datum on which the choice between hypotheses H_0 and H_1 is based. It will have a Poisson distribution with different mean values under the two hypotheses, and in order to attain a pre-assigned false-alarm probability, randomization will in general be necessary.[16]

Applying this scheme to detecting the Gaussian image given by (37), we assume that we count all the photoelectrons emitted from a circle of radius $\rho\Sigma$ centered at the origin. Under hypothesis H_0 the mean number of counts is

$$\underset{\sim}{E}(n|H_0) = n_0 = \pi M_0 \rho^2 \Sigma^2 = \frac{1}{2} \rho^2 N_0, \tag{53}$$

where N_0 is given by (38). Under H_1 the mean number is

$$\underset{\sim}{E}(n|H_1) = n_1 = \iint_{|\underset{\sim}{x}|<\rho\Sigma} M_1(\underset{\sim}{x}) d^2\underset{\sim}{x} = N_0\left[\frac{1}{2} \rho^2 + D^2 (1 - e^{-\rho^2/2}) \right], \tag{54}$$

where $D^2 = N_s/N_0$ is the signal-to-noise ratio. The detector chooses hypothesis H_1 whenever the number n of counts exceeds an integer θ; H_0 is chosen when $n < \theta$; but when $n = \theta$, H_1 is chosen with probability f. The false-alarm and detection probabilities are then

$$Q_0 = \exp(-n_0) \left[f n_0^{\theta}/\theta! + \sum_{n=\theta+1}^{\infty} n_0^n/n!\right],$$

$$Q_d = \exp(-n_1) \left[f n_1^{\theta}/\theta! + \sum_{n=\theta+1}^{\infty} n_1^n/n!\right]. \tag{55}$$

In Figs. 3 and 4 the probability of detection so calculated is plotted versus the mean number N_s of photoelectrons ejected by the Gaussian image, for $Q_0 = 10^{-3}$ and 10^{-5}. For each point on the curve the value of ρ was varied to yield maximum detection probability. The maxima are quite flat, and the radius $\rho\Sigma$ of the counting area is not critical. The values of ρ used are listed in Table I.

When the average error probability in (9) is to be minimum, the likelihood ratio $\Lambda(n)$ formed from the number n must be compared with the decision level $\Lambda_0 = \zeta/(1 - \zeta)$, and hypothesis H_1 is chosen when $\Lambda(n) > \Lambda_0$. Thus the image sought is declared present whenever

$$n > \left\{ \ell n[\zeta/(1 - \zeta)] + n_1 - n_0 \right\} / \ell n(n_1/n_0);$$

otherwise hypothesis H_0 is chosen. The average probability of error as given by (9) can then be calculated by summing Poisson probabilities, and it has been plotted as the dashed curves in Fig. 5 at $\zeta = \frac{1}{2}$. For each point on the curve the value of ρ was chosen to yield minimum error probability.

6. Conclusions

From Figs. 3, 4, and 5 we see that the ideal photoelectric detector and the threshold detector, which utilize information about the shape of the image $J_s(\underset{\sim}{x},\nu)$, are hardly better than the simple counter when the effective area of this is selected to yield maximum detection probability Q_d or minimum error probability P_e. If the image has a uniform distribution

over a finite area I' of the image plane, outside of which it vanishes, all three detectors are basically identical. Because the ideal photoelectric detector is nearly equivalent to the optimum detector of an incoherently radiating object in the presence of thermal background light when it has unit quantum efficiency and diffraction is insignificant, there is little one can do to improve the simple counter except to increase its quantum efficiency; registering the points of emission of the photoelectrons does not help much to increase the reliability of detecting an image.

REFERENCES

1. C. W. Helstrom, "The detection and resolution of optical signals", IEEE Transactions on Information Theory, vol. IT-10, pp. 275-287; October, 1964.
2. C. W. Helstrom, Statistical Theory of Signal Detection, 2nd ed., Pergamon Press, Oxford; 1968. See p. 188.
3. C. W. Helstrom, "Detection of incoherent objects by a quantum-limited optical system", J. Opt. Soc. Am. vol. 59, pp. 924-936; August, 1969.
4. C. W. Helstrom, "Quantum detection theory" in Progress in Optics, E. Wolf, ed., vol. 10, pp. 291-369; 1972. See §5.1, pp. 334-338.
5. C. W. Helstrom, "Modal decomposition of aperture fields in detection and estimation of incoherent objects", J. Opt. Soc. Am. vol. 60, pp. 521-530; April, 1970.
6. Ref. 4, §5.4.2, pp. 357-359.
7. U. Grenander, G. Szegö, Toeplitz Forms and Their Applications, University of California Press; 1958. See also §8.6, pp. 136-139.
8. C. W. Helstrom, "Detection and resolution of incoherent objects seen through a turbulent medium", J. Opt. Soc. Am. vol. 59, pp. 331-341; March, 1969.
9. W. Feller, An Introduction to Probability Theory and Its Applications, J. Wiley & Sons, Inc., New York; 1966, vol. 2, ch. 17, pp. 526-563.
10. B. V. Gnedenko, The Theory of Probability, Chelsea Publishing Co., New York; 1967, ch. 9, pp. 319-340.

11. E. J. Farrell, "Information content of photoelectric star images", J. Opt. Soc. Am. vol. 56, pp. 578-587; May, 1966.

12. H. E. Daniels, "Saddlepoint approximations in statistics", Ann. Math. Stat. vol. 25, pp. 631-650; September, 1954.

13. S. O. Rice, "Uniform asymptotic expansions for saddle point integrals - application to a probability distribution occurring in noise theory", Bell System Tech. J., vol. 47, pp. 1971-2013; November, 1968.

14. L. Wang, "Numerical calculation of cumulative probability from the moment-generating function", Proceedings of the IEEE (in press).

15. Ref. 2, pp. 160-161.

16. Ref. 4, §1.2, pp. 295-297.

TABLE I

Optimum Radius for Simple Counter

$N_0 = 0.5$

N_s	$\rho(Q_0 = 10^{-3})$	$\rho(Q_0 = 10^{-5})$
1	1.31	1.37
2	1.72	1.68
4	1.72	1.68
8	2.10	1.68
12	2.10	1.98
20	2.10	1.98
24	2.46	2.28

$N_0 = 5$

N_s	$\rho(Q_0 = 10^{-3})$	$\rho(Q_0 = 10^{-5})$
1	1.36	1.37
2	1.44	1.44
4	1.60	1.58
8	1.60	1.58
12	1.75	1.65
20	1.82	1.78
24	1.82	1.78

FIGURE CAPTIONS

Fig. 1. False-alarm probability Q_0 and detection probability Q_d as a function of decision level g_0 for ideal photoelectric detector as calculated by the saddlepoint, Gaussian, and gamma approximations; $N_0 = N_s = 5$.

Fig. 2. Progress of the saddlepoint s_0 of the phase of the integrand of (42) as a function of the signal-to-noise ratio D^2; $N_0 = 0.5$ and 5, $Q_0 = 10^{-3}$ and 10^{-5}.

Fig. 3. Probability Q_d of detection of a Gaussian image vs. the mean number N_s of photoelectrons ejected by the image; $Q_0 = 10^{-3}$. Curves are indexed by the noise parameter N_0 defined in (38).

Fig. 4. Probability Q_d of detection of a Gaussian image vs. the mean number N_s of photoelectrons ejected by the image; $Q_0 = 10^{-5}$. Curves are indexed by the noise parameter N_0 defined in (38).

Fig. 5. Average error probability P_e in deciding between presence and absence of Gaussian image when these have equal prior probabilities, vs. mean number N_s of photoelectrons ejected by the image. Curves are indexed by the noise parameter N_0 defined in (38).

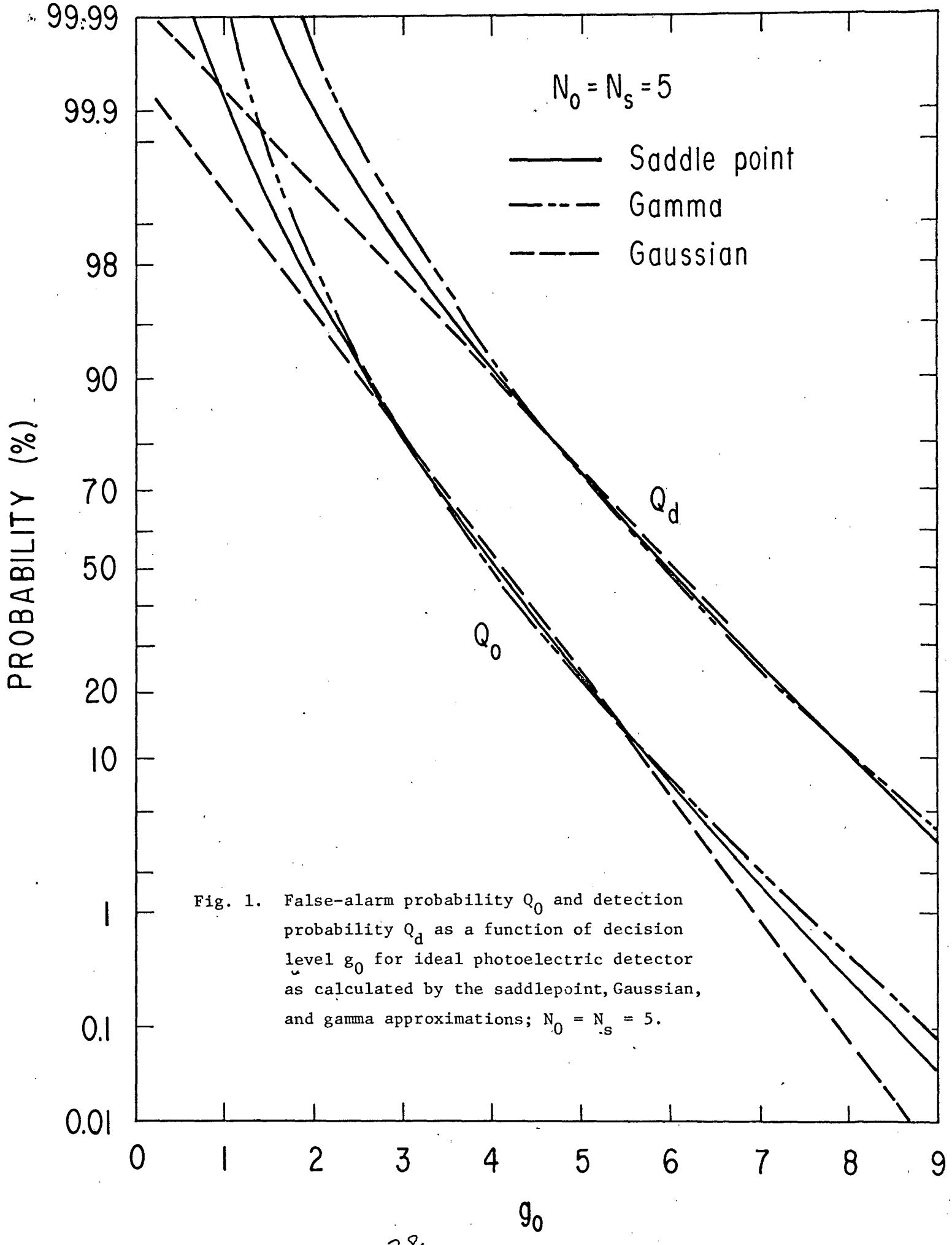

Fig. 1. False-alarm probability Q_0 and detection probability Q_d as a function of decision level g_0 for ideal photoelectric detector as calculated by the saddlepoint, Gaussian, and gamma approximations; $N_0 = N_s = 5$.

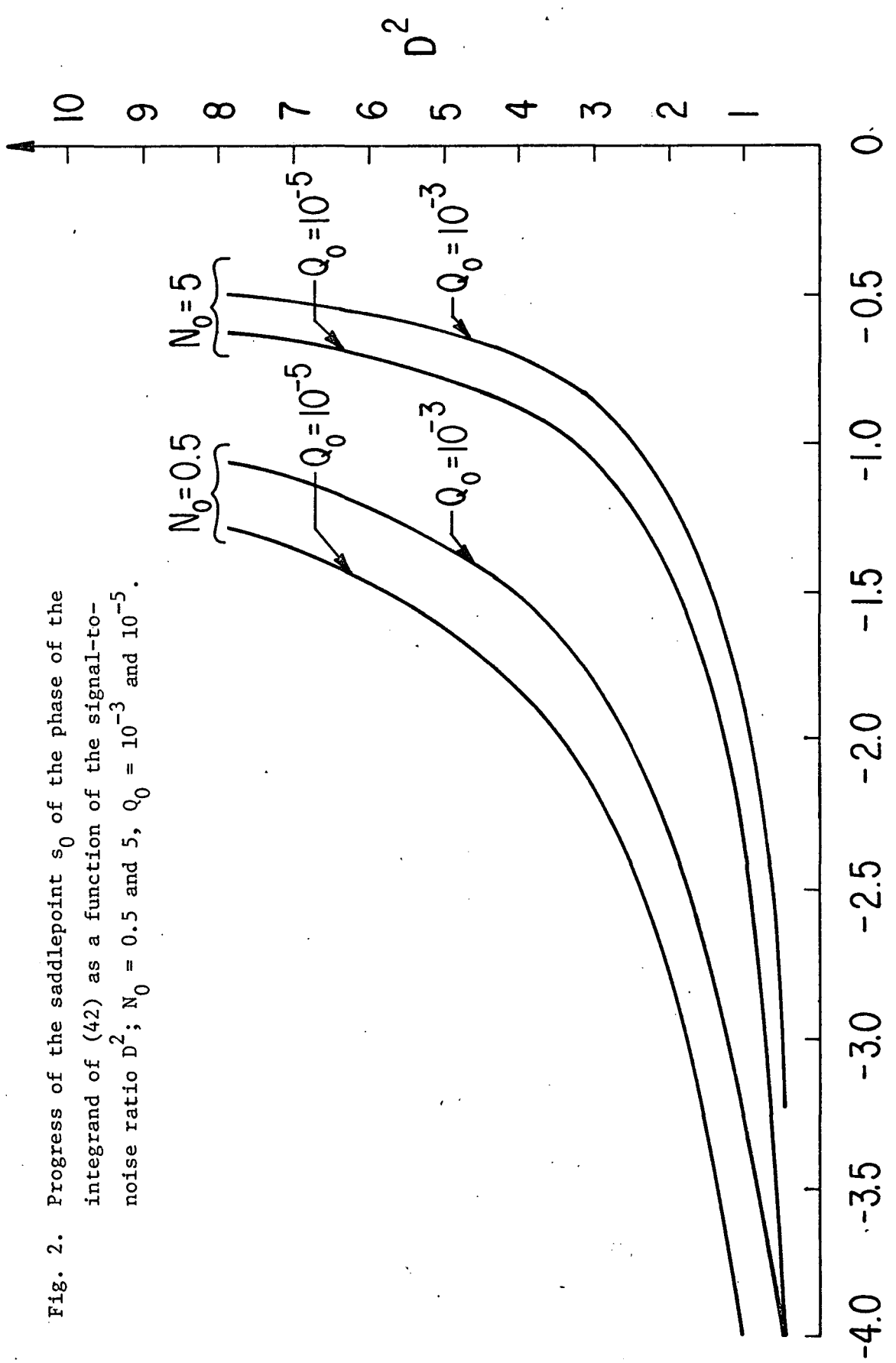

Fig. 2. Progress of the saddlepoint s_0 of the phase of the integrand of (42) as a function of the signal-to-noise ratio D^2; N_0 = 0.5 and 5, Q_0 = 10^{-3} and 10^{-5}.

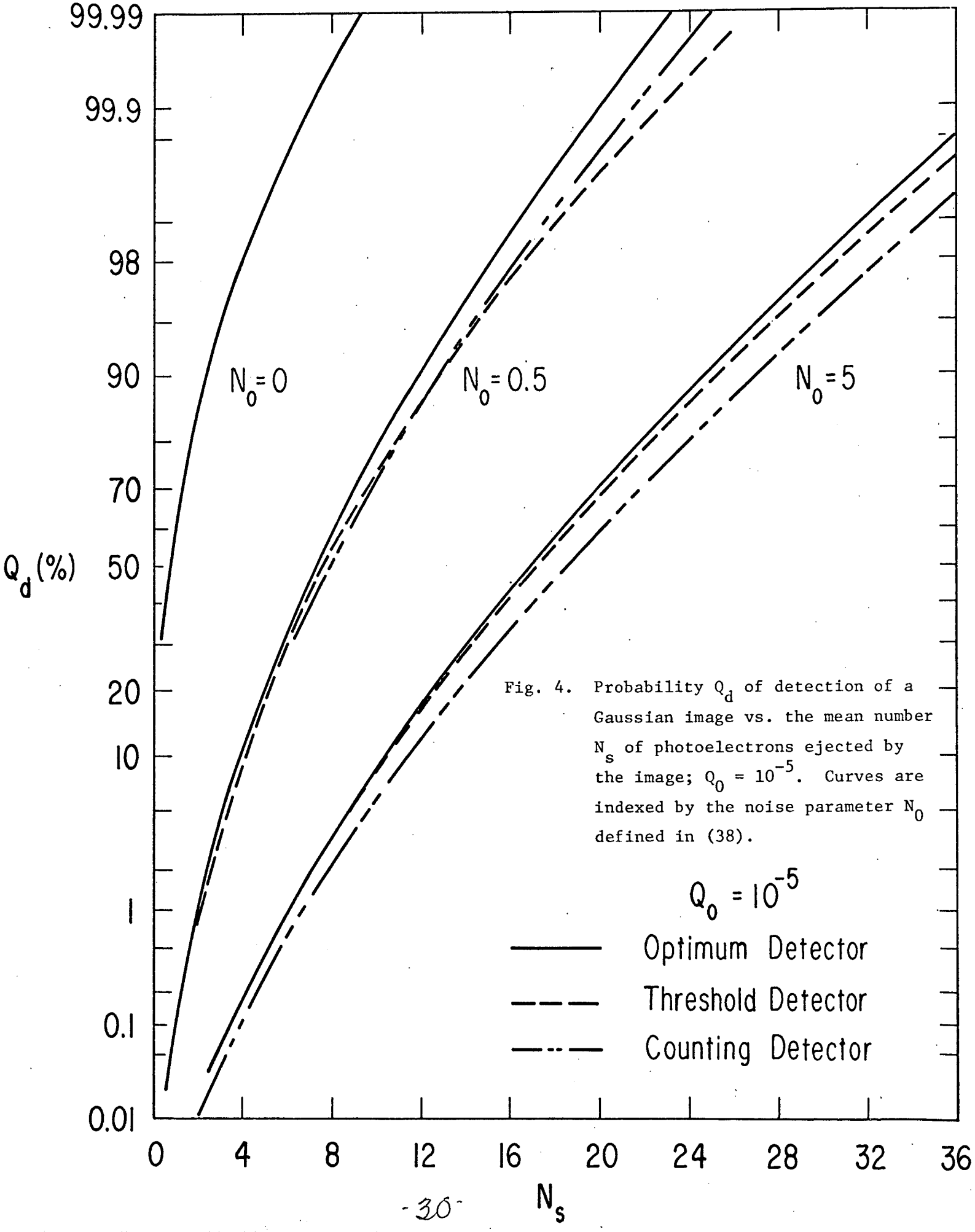

Fig. 4. Probability Q_d of detection of a Gaussian image vs. the mean number N_s of photoelectrons ejected by the image; $Q_0 = 10^{-5}$. Curves are indexed by the noise parameter N_0 defined in (38).

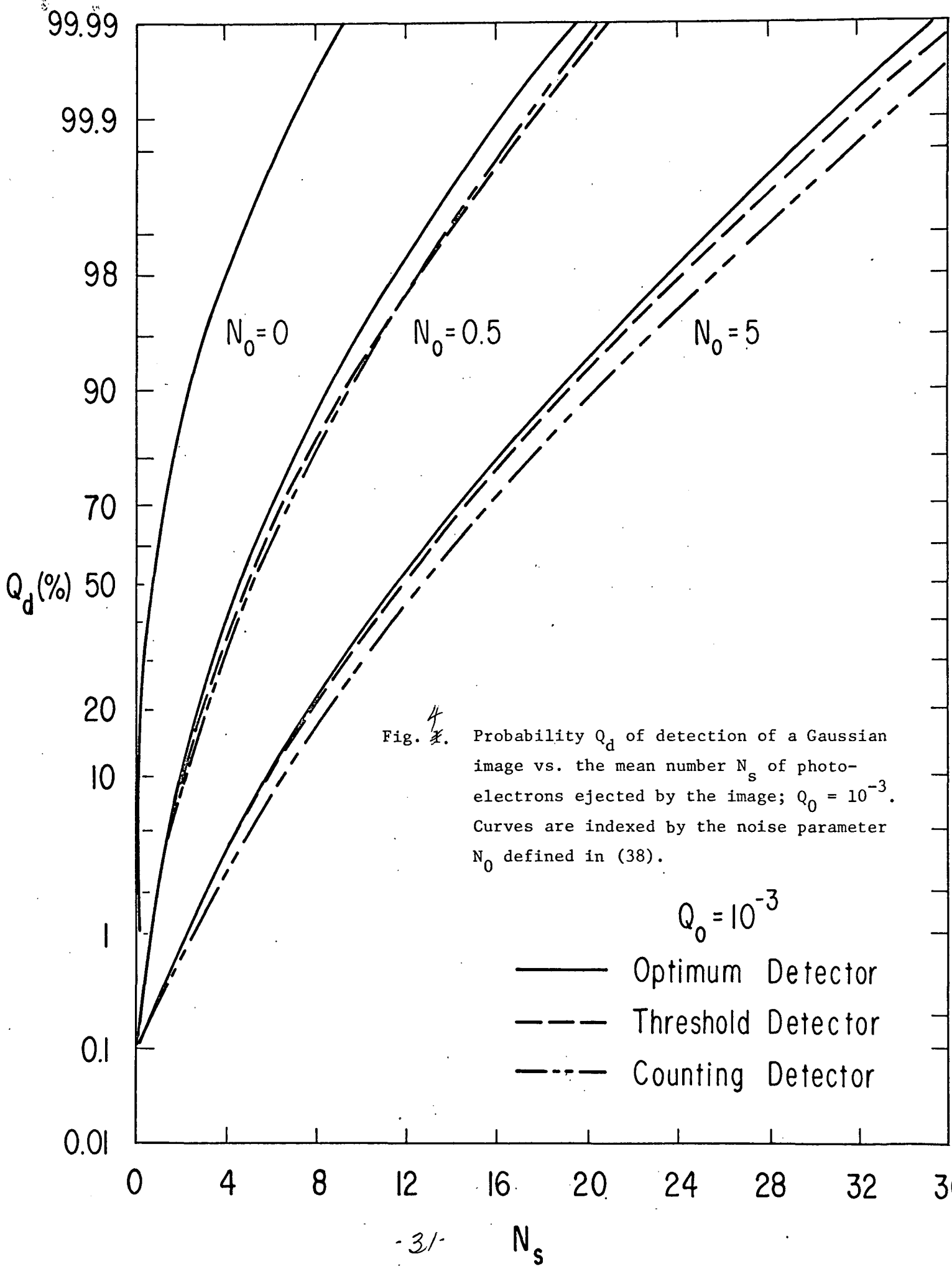

Fig. 4. Probability Q_d of detection of a Gaussian image vs. the mean number N_s of photoelectrons ejected by the image; $Q_0 = 10^{-3}$. Curves are indexed by the noise parameter N_0 defined in (38).

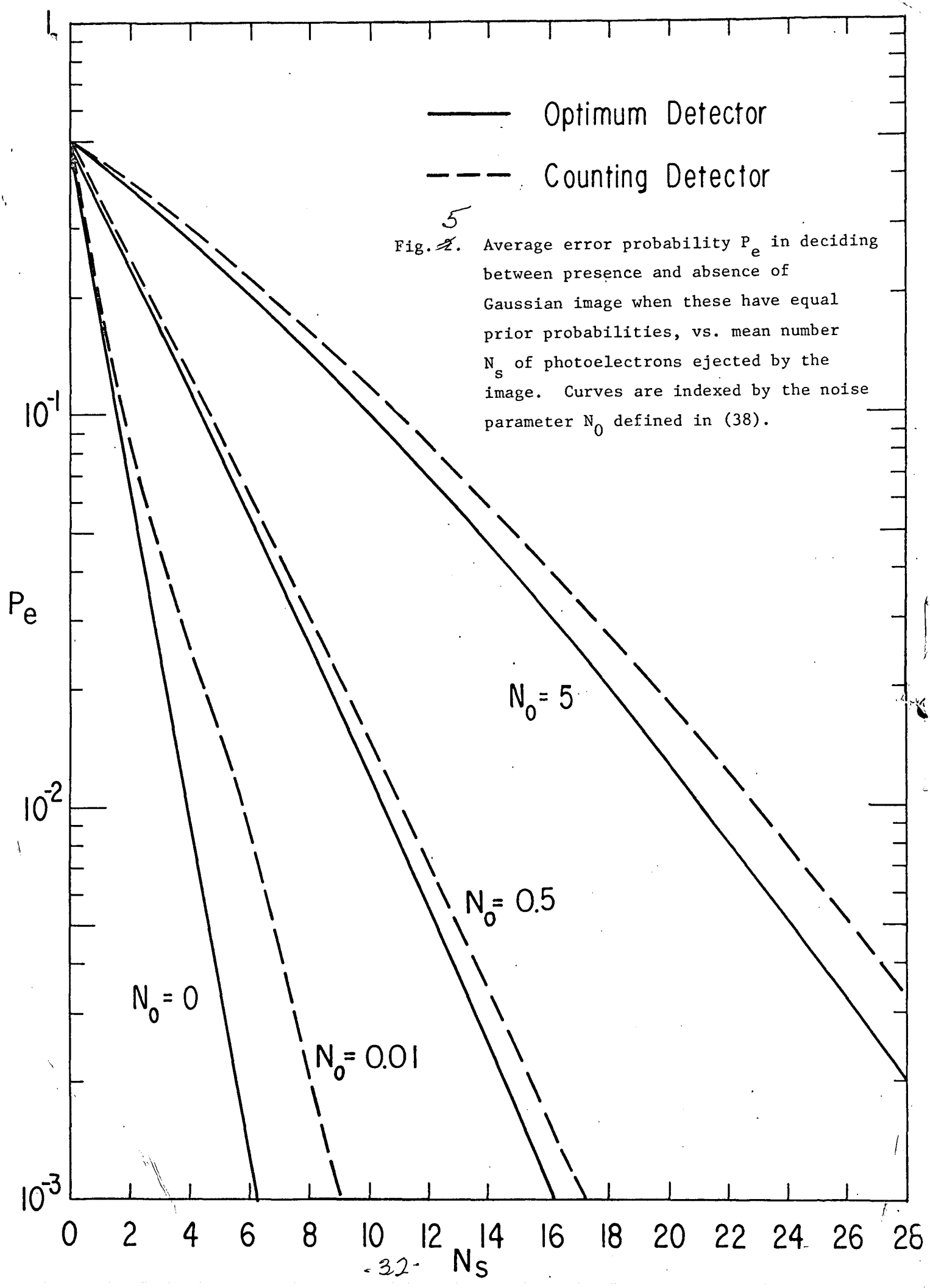

Fig. 5. Average error probability P_e in deciding between presence and absence of Gaussian image when these have equal prior probabilities, vs. mean number N_s of photoelectrons ejected by the image. Curves are indexed by the noise parameter N_0 defined in (38).